Author's Accepted Manuscript

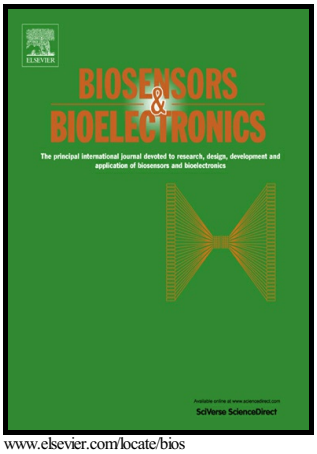

www.elsevier.com/locate/bios

The detection of brucellosis antibody in whole serum based on the low-fouling electrochemical immunosensor fabricated with magnetic Fe_3O_4@Au@PEG@HA nanoparticles

Shuli Lv, Jinliang Sheng, Shiyi Zhao, Mingchao Liu, Lihua Chen

PII: S0956-5663(18)30440-8
DOI: https://doi.org/10.1016/j.bios.2018.06.010
Reference: BIOS10530

To appear in: *Biosensors and Bioelectronic*

Received date: 13 April 2018
Revised date: 3 June 2018
Accepted date: 5 June 2018

Cite this article as: Shuli Lv, Jinliang Sheng, Shiyi Zhao, Mingchao Liu and Lihua Chen, The detection of brucellosis antibody in whole serum based on the low-fouling electrochemical immunosensor fabricated with magnetic Fe_3O_4@Au@PEG@HA nanoparticles, *Biosensors and Bioelectronic,* https://doi.org/10.1016/j.bios.2018.06.010

The detection of brucellosis antibody in whole serum based on the low-fouling electrochemical immunosensor fabricated with magnetic Fe_3O_4@Au@PEG@HA nanoparticles

Shuli Lv [a,12], Jinliang Sheng [b,1,2], Shiyi Zhao [a2], Mingchao Liu [a2], Lihua Chen [a, b,*2]

[a] Key Laboratory of Sensor Analysis of Tumor Marker, Ministry of Education, Key Laboratory of Biochemical Analysis, Shandong Province, College of Chemistry and Molecular Engineering, Qingdao University of Science and Technology, 266042, Qingdao, China.

[b] Key Laboratory of Prevention and Control of Animal Disease of Xinjiang Corps. College of Animal Science and Technology, Shihezi University, 832000, Shihezi, Xinjiang, China.

*Corresponding author: Lihua Chen, E-mail: lihuachen@qust.edu.cn.; Fax: +86 53284022681; Tel: +86 15054246089.

[1] These authors contributed equally to this work.

[2] These universities contributed equally to this work.

Abstract

It is a novel competitive challenge for electrochemical biosensor to directly, rapidly and ultrasensitively detect the disease markers in the whole serum due to biofouling caused by the complexity of actual samples. In this paper, poly (ethylene glycol) (PEG) and hyaluronic acid (HA) were utilized to modify Fe_3O_4@Au nanoparticles (NPs). Based on the successfully preparation and characterization of Fe_3O_4@Au@PEG@HA NPs with TEM, SEM, XRD, FTIR and EDS, respectively, a novel immunosensor of brucellosis with high selectivity, sensitivity and almost perfect protein-resistant properties in various external environments, especially, in complex biological systems was fabricated. More importantly, this immunosensor is capable of assaying brucellosis antibody in 100% serum without suffering from any significant biological interference. In addition, a wide linear response range from 10^{-15} g mL^{-1} to 10^{-11} g mL^{-1} towards antibody in 100 % serum and a low limit of detection (LOD) of 0.36 fg mL^{-1} (3σ, n=13) are demonstrated, which indicates that this immunosensor has a promising potential in clinical diagnosis.

Key words: Fe_3O_4@Au NPs; hyaluronic acid; brucellosis; antifouling; immunosensor

1. Introduction

Brucellosis, a zoonotic disease, poses a great threat to veterinary and public health in many developing countries. (Ghasemi et al., 2014) People may be transmitted by eating unsterilized dairy products or directly contacting with diseased animals. Although vaccines are the most efficacious and economical way of controlling brucellosis, a completely effective and safe vaccine is unavailable for both human and animals. (Li et al., 2017) Therefore, developing a sensitive and rapid detection method for brucellosis in complex biological system is of great significance.

Numerous techniques for the detection of brucellosis antibodies have been developed, (Kuila et al., 2017; Ghodasara et al., 2010; Abdel-Hamid et al., 2017) ranging from plate agglutination test (PAT), tiger red plate agglutination test (RBPT) to standard test tube agglutination test (SAT). However, these traditional methods may suffer from cross reactions, false positives or false negatives, which are possible to procrastinate the time of the correct diagnosis, therefore, result in the complexity of follow-up treatment methods. Ultimately, this disease will not be cured. Now polymerase chain reaction (PCR) and enzyme-linked immunosorbent assay (ELISA) as a new supplementary detection technology has been widely used due to their excellent sensitively and accurately, but complex pretreatment and the requirement of professional executor and expensive instrument restricts their further development.

Electrochemical bioanalytical technique has become increasingly important in

biological assays due to its simple instrumentation, lower cost, fast response time and portability, especially its excellent sensitivity (10^{-19} g mL^{-1})(Gong et al., 2016). However, the actual sample composition is very complex and contains various proteins, organic and inorganic compound. If the interface of sensor covers with a layer of non-specific proteins, it will mask the analytic signal and greatly reduce the accuracy of the sensors. More unfortunately, for early infected patients with brucella, the antibodies in the blood are very low. Only after one month, a peak value (10^{-7} g mL^{-1}) will appear. So, direct, accurate and ultrasensitive detection of the brucellosis antibody in the whole serum of early infected patients holds great promise to improve the cure rate of patient. Until now, electrochemical sensing has solved the problem of high selectivity and high sensitivity detection of disease markers, but only few reports demonstrated rapid diagnosis of disease in 100 % serum. Therefore, many efforts were dedicated to constructing a sensor with an excellent antifouling interface. (Hui et al., 2017; Cui et al., 2017)

Nevertheless, a prominent contradiction is that the excessive chemical modification of sensor interface may lead to the deterioration of sensor conductivity. So preparation of materials that not only possess high conductivity but also exhibit high anti-fouling properties as an important work is investigated in our experiment. Magnetic core-shell Fe_3O_4@Au nanoparticles (NPs) have been extensively used to fabricate bio-electrochemical interfaces for biosensors. One case is that Yao et al used Fe_3O_4@Au NPs to fabricate an ultrasensitive and highly specific electrochemical aptasensor for thrombin determination. (Zhao et al., 2011) Another case is that Hao et

al successfully constructed a novel electrochemiluminescence immunosensor based on Fe_3O_4@Au NPs and glucose oxidase (GOD)-labeled antigen, which exhibited high sensitivity and a wide linear range for Bacillus thuringiensis Cry1Ac. (Li et al., 2013) The excellent conductivity of the gold shell is well known. Simultaneously, the excellent biocompatibility of Fe_3O_4@Au NPs endows this material with a performance of chemical modification, therefore, lays the foundation of its excellent anti-fouling properties.

Here, on the basis of poly(ethylene glycol) (PEG) coated Fe_3O_4@Au NPs (Fe_3O_4@Au@PEG NPs), hyaluronic acid (HA) modified Fe_3O_4@Au@PEG NPs (Fe_3O_4@Au@PEG@HA NPs) were synthesized and further used to construct brucellosis immunosensor. As we expected, interface platform of Fe_3O_4@Au@PEG@HA NPs modified electrode demonstrated both the excellent conductivity and the almost perfect antifouling properties in a variety of external environment, especially in complex biological systems. The percent change of DPV current response of Fe_3O_4@Au@PEG@HA NPs modified electrodes before and after incubation with 100 % serum is only 5.19 %. In addition, this sensor modified with OMP31 (members of the brucella outer membrane proteins) (Zheng et al., 2015) showed a good linear correlation with the concentration of brucellosis antibody in 100 % serum ranging from 10^{-15} g mL^{-1} to 10^{-11} g mL^{-1}, and the detection limit was as low as 0.36 fg mL^{-1} (3σ, n=13). All results indicated its great potential diagnostic applications in clinical of brucellosis.

2. Materials and Methods

2.1. Chemicals and Instrument

Gold chloride hydrate ($HAuCl_4 \cdot XH_2O$), bovine serum albumin (BSA, MW: 66.43 KDa) were supplied by Aladdin Reagents (Shanghai, China). Nhydroxysuccinimide (NHS), carbodiimide hydrochloride (EDC), 1,4-butanediol diglycidyl ether (BDE), hexaammineruthenium (III) chloride ($Ru(NH_3)_6^{3+}$) were purchased from Sigma-Aldrich. Iron (III) chloride hexahydrate ($FeCl_3 \cdot 6H_2O$), iron (II) chloride tetrahydrate ($FeCl_2 \cdot 4H_2O$) were purchased from Sinopharm Chemical Reagent Co., Ltd. PEG terminated with amino group (molecular weights of 5000 g mol^{-1}) was purchased from Shanghai Yare Biotech, Inc. Hyaluronic acid (MW: 1200 KDa) was obtained from Shanghai yuanye Biological technology Co., Ltd., Helper phage (M13KO7, 1.0×10^{11} pfu mL^{-1}) was obtained from New England BioLabs, Inc. (Ipswich, MA, USA). Cow milk with a protein concentration of about 30 mg mL^{-1} was from Yili Industrial Co. and purchased in a local market. BP26 protein, VirB5 protein, OMP31 protein, brucellosis antibody and serum were donated by college of animal science and technology, Shihezi University. All other chemicals were analytical grade quality and were used without further purification. Phosphate buffered saline (PBS, 10 mM, pH 7.4, containing 0.9 % NaCl) were used in all experiments. All aqueous solutions were prepared with pure water produced by a Milli-Q water purifying system. All experiments were performed at ambient room temperature.

Transmission electron microscopy (TEM) was performed with a JEM-2100 TEM instrument (Hitachi High-Technology Co., Ltd. Japan). Scanning electron microscopy

(SEM) was fulfilled with a JEOL JSM-7500F SEM instrument (Hitachi High-Technology Co., Ltd. Japan) to characterize nanostructures and morphologies of different magnetic NPs. Fourier transform infrared spectroscopy (FTIR) was performed with the Bruker Tensor 70 spectrometer (Bruker Optics, Germany). Contact angle measurements (CA) were carried out using a JC2000C1 goniometer (Shanghai Zhongchen instrument Co., Ltd. China). Magnetic properties of all samples were measured with vibrating sample magnetometer (VSM) (equipped with physical property measurement system (PPMS)) with a maximum applied continuous field of 15 000 Oe at room temperature.

All the electrochemical measurements were carried out with a CHI660E electrochemical workstation (Shanghai Chenhua Instrument Co. Ltd., China). A conventional three-electrode system was employed with a magnetic glass carbon electrode as working electrode (MGCE, 3.0 mm in diameter), a platinum wire as auxiliary electrode and saturated calomel electrode as reference electrode. The magnetic glass carbon electrode was composed by a copper connector, a hollow cylinder magnet and a poly tetra fluoroethylene cylindrical tube packed with glass carbon. CV of the bare electrode and the modified electrodes were recorded in PBS (10 mM, pH 7.4) doped with 5.0 mM $Ru(NH_3)_6^{3+}$ and 0.1 M KCl. And its parameters were as follows: scanning range from -0.6 to 0.2 V with scan rate of 0.10 V/s

2.2. Preparation of Fe_3O_4@Au@PEG@HA NPs

The core-shell magnetic Fe_3O_4@Au NPs were synthesized by chemical co-precipitation methods as reported. (Lyon and Fleming, 2004; Zhao et al., 2008)

Then the PEG and HA were modified on Fe_3O_4@Au NPs surface, the detail procedures are illustrated as follows.

The freshly-prepared Fe_3O_4@Au NPs (5 mL, 2 mg mL^{-1}) were mixed with equal volume of 4-arm-NH_2-PEG (4 mM) (Figure S1A) and stirred for 48 h at 4 ℃. After incubation of two days, free PEG was removed by washing Fe_3O_4@Au@PEG NPs several times with water. Subsequently, Fe_3O_4@Au@PEG NPs were dropped into a mixture containing HA (4 mg mL^{-1}), EDC (20 mg mL^{-1}) and NHS (20 mg mL^{-1}) for 72 h at room temperature. The successfully-prepared Fe_3O_4@Au@PEG@HA NPs were collected and washed with water and then re-dispersed in 2.5 mL deoxygenated water for further use.

2.3. The construction of Fe_3O_4@Au@PEG@HA NPs modified sensor

Magnetic glassy carbon electrodes (MGCEs) were firstly polished with alumina slurries and ultrasonically washed. Next, MGCEs were dried with nitrogen and immersed into Fe_3O_4@Au@PEG@HA NPs (300 μL, 1mg mL^{-1}) for 30 min. Subsequently, they were dried in a constant-temperature oven at 37 °C for 1 h, then rinsed with water, and stored in water at 4 °C for electrochemically measured.

2.4. Nonspecific protein adsorption of Fe_3O_4@Au@PEG@HA NPs modified sensor

To evaluate the antifouling performance of interface platform of Fe_3O_4@Au@PEG@HA NPs modified sensor, different samples including BSA (10 mg mL^{-1}, dissolved with PBS solution), helper phage (M13KO7, diluted to 1.0×10^8 pfu mL^{-1} with PBS), 100 % cow milk, 100 % serum and a series concentrations of serum (1 %, 5 %, 10 %, 20 % and 50 % (V/V), diluted with PBS) were tested using

DPV techniques of CHI660E. The DPV responses of Fe_3O_4@Au@PEG@HA NPs modified electrodes before and after incubation with single protein solution or complex media for 60 min were recorded and the changes of the peak current were compared. DPV measurements were carried out in PBS (10 mM, pH 7.4) doped with 5.0 mM $Ru(NH_3)_6^{3+}$ and 0.1 M KCl, and its parameters were as follows: potential increment of 4.0 mV, pulse amplitude 50 mV, pulse width (modulation time) 50 ms, pulse period (interval) 500 ms.

2.5. Immobilization of OMP31

As shown in scheme 1A, electrodes modified with Fe_3O_4@Au@PEG@HA NPs (MGCE/Fe_3O_4@Au@PEG@HA NPs) were incubated in 300 μL solution of BDE (0.6 M, diluted with 10 mM carbonate buffer solution with pH of 9.5) for 12 h, then immersed in 300 μL carbonate buffer (10 mM, pH 9.5) containing 1 μg mL^{-1} OMP31 for another 12 h (Figure S1B). Finally, OMP31 modified electrode was thoroughly washed with PBS and stored in PBS for further use.

2.6. Detection of brucellosis antibody

PBS solutions (30 μL, pH 7.4) containing different concentrations of brucellosis antibody were dropped on the interface of the prepared immunosensor for 60 min. The DPV peaks before and after the completion of specific binding between antigen and antibody were measured. All of experiments were carried out in PBS (10 mM, pH 7.4) doped with 5.0 mM $Ru(NH_3)_6^{3+}$ and 0.1 M KCl. And its parameters were as follows: potential increment of 4.0 mV, pulse amplitude 50 mV, pulse width (modulation time) 50 ms, pulse period (interval) 500 ms.

3. Results and discussions

3.1. The choice of materials and the construction of immunosensor

Here, a novel Fe_3O_4@Au@PEG@HA NP was successfully prepared and applied to build immunosensor of brucellosis as shown in scheme 1. Fe_3O_4@Au NPs were used as the base due to its excellent conductivity and biocompatibility. Then, PEG terminated with amine was directly grafted on the surface of Fe_3O_4@Au NPs by Au-N bond. As we known, C-O-C group from PEG can form a dense hydrated layer to protect the surfaces from nonspecific adsorption of proteins and prevent nanoparticle agglomeration. However, the protein-repellent nature of PEG modified interface strongly depends on the density of PEGylation. (Gref et al., 2000; Michel et al., 2005) Unfortunately, the curvature of the NPs has a serious influence on the PEG density modified on surface. Therefore PEG modified magnetic NPs only show a decrease adsorption against nonspecific protein to a certain extent (Xie et al., 2007; Feng et al., 2008), rather than the “zero” protein adsorption, which is consistent with the result of our previous antifouling experiment (Figure S2). In addition, PEG is sensitive to oxidation. (Ostuni et al., 2001; Cui eh al., 2014; Yu and Frey, 2015) Thus, it is urgent to choose another material to make up for the shortages of PEG.

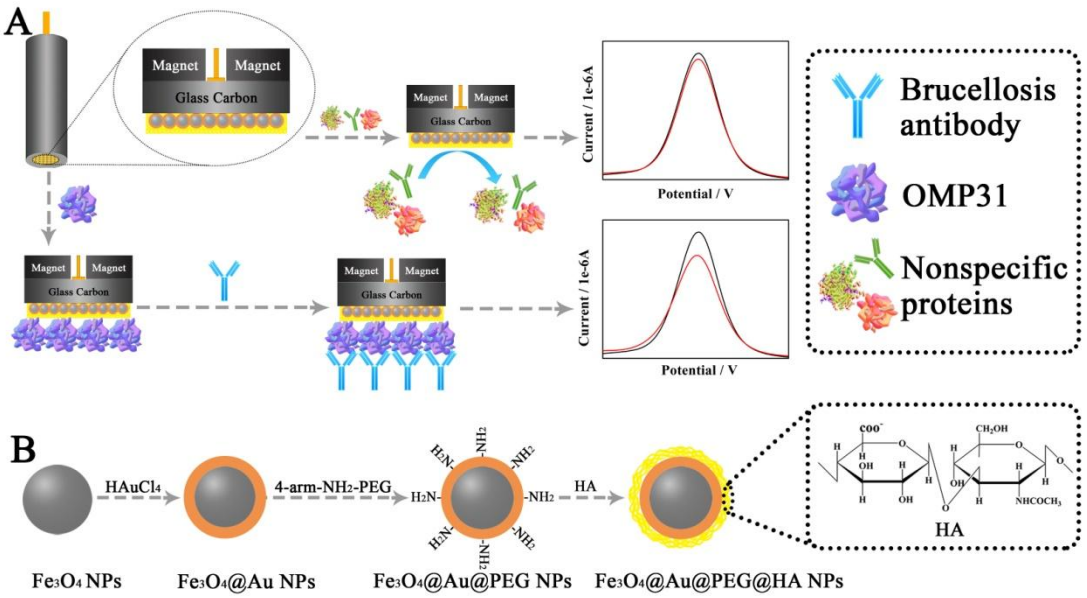

Scheme 1. A: Illustration of the fabrication of electrochemical immunosensor of brucellosis; B: Illustration of the fabrication of Fe_3O_4@Au@PEG@HA NPs.

Charged polypeptide and zwitterionic polymers are out of our consideration because of high price or the cumbersome chemical modification process. Polysaccharide successfully attracted our attention due to its excellent bio-inertness, biocompatibility and rich source. Hyaluronic acid (HA), one of the polysaccharides, contains quite a few of hydrogen bond donors/acceptors groups such as hydroxyl groups (-OH), amide (CO-NH) and carboxyl groups (COOH) (Li et al., 2014; Dosio et al., 2016), whose protein-resistant performance has been proved very well in previous literature. For instance, SPR sensor chips fabricated with HA have demonstrated the excellent antifouling capabilities against single protein and complex samples, including these interface platform based on the MUO/HA (11-mercapto-1-undecanol/hyaluronic acid) (Liu et al., 2014), HADA-GSH (polyanion of the hyaluronic acid-dopamine conjugate with a reduced glutathione) (Huang et al., 2015) and PDA/HA (polymerization of dopamine and the simultaneous

deposition of hyaluronic acid) (Ye et al., 2016) matrices. Here, HA was anchored on the Fe_3O_4@Au@PEG NPs through covalent bond. The carboxyl groups from HA molecules react with EDC/NHS to produce an active ester (O-acylisourea)-leaving group, which can more effectively covalently bond to the primary amine of PEG to form a peptide bond on the surface of Fe_3O_4@Au@PEG NPs. (Zhang et al., 2006) Subsequently, the successfully fabricated Fe_3O_4@Au@PEG@HA NPs were magnetically adsorbed onto the magnetic glass carbon electrode as substrate. Interestingly, during the investigation on antifouling performance of surface platform of sensor, ideal protein resistance results were demonstrated (the detail information was discussed in 3.3). Next, OMP31 generally considered as the diagnostic tools for brucellosis antibody detection was conjugated with Fe_3O_4@Au@PEG@HA NPs modified sensor by ring-opening reactions between epoxy of BDE and amino groups of OMP31 under basic condition. As expected, the fabricated immunosensor exhibited favorable selectivity and high sensitivity. Most importantly, it was capable of assaying brucellosis antibody in 100 % serum.

3.2. Characterization of Fe_3O_4@Au@PEG@HA NPs

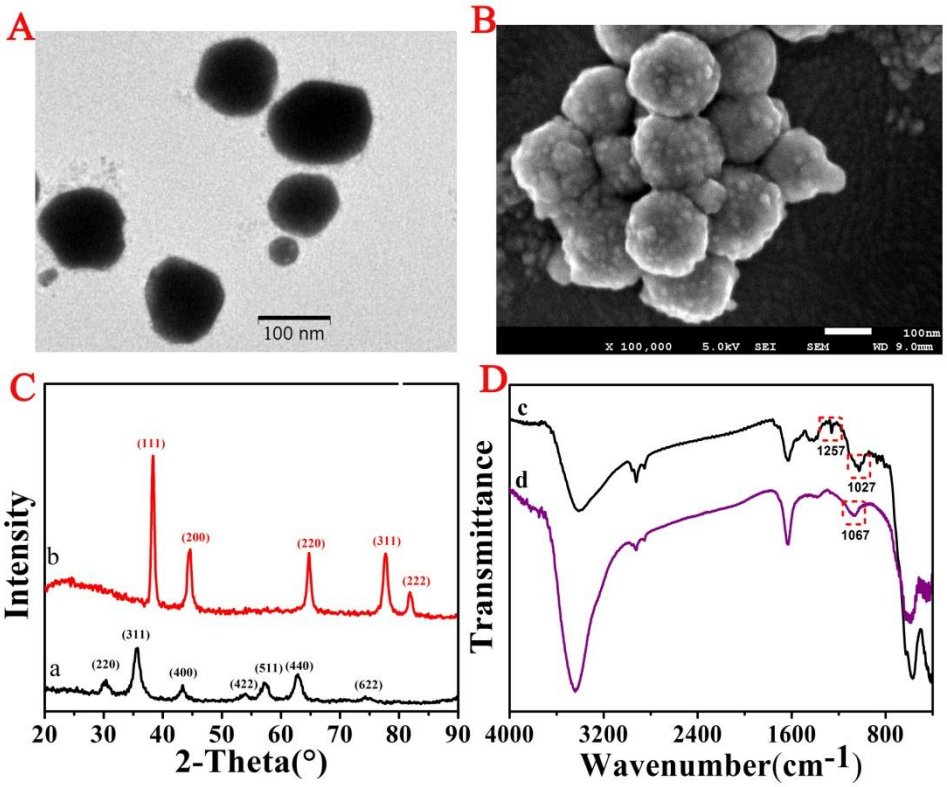

Figure 1. A: TEM image of Fe_3O_4@Au@PEG@HA NPs; B: SEM image of Fe_3O_4@Au@PEG@HA NPs; C: X-ray diffractograms of (a) Fe_3O_4 NPs and (b) Fe_3O_4@Au NPs; D: FTIR spectral of (c) Fe_3O_4@Au@PEG NPs, (d) Fe_3O_4@Au@PEG@HA NPs.

The morphology, size and structure of Fe_3O_4@Au@PEG@HA NPs were successfully characterized by TEM (Figure 1A), SEM (Figure 1B), XRD (Figure 1C), FTIR (Figure 1D) and EDS (Figure S3) one by one. As shown in TEM and SEM images, the Fe_3O_4@Au@PEG@HA NPs displayed uniformly spherical structure with a mean diameter of 120 nm and dispersed well with no signs of aggregation.

In XRD patterns of Fe_3O_4 NPs (Figure 1C, curve a), curve presents seven peaks (30.42°, 35.52°, 43.38°, 53.80°, 57.15°, 62.80° and 74.39°) which correspond to the (220), (311), (400), (422), (511), (440) and (622) diffraction peaks of ferrites (JCPDS no. 19-0629). In XRD patterns of Fe_3O_4@Au NPs (Figure 1C, curve b), only five

diffraction peaks are presented at 38.41°, 44.62°, 64.87°, 77.69° and 81.82°, respectively, which are indexed as the (111), (200), (220), (311) and (222) diffraction peaks of Au crystal with a cubic phase (JCPDS no. 04-0784). The reason that peaks associated with magnetite disappeared may be that the diffraction from Fe_3O_4 is too weak to be detected due to the heavy atom effect of Au. (Xu et al., 2007)

In FTIR analysis, the spectrum of Fe_3O_4@Au@PEG NPs (Figure 1D, curve c) shows several characteristic peaks of PEG. The peak at 3406 cm^{-1} is attributed to -NH_2 stretching. The peaks at 2923 cm^{-1} and 2853 cm^{-1} are ascribed to -CH_2. The peak at 1630 cm^{-1} is caused by in-plane bending vibration of -NH_2 group. The peaks at 1257 cm^{-1} and 1027 cm^{-1} correspond to the symmetrical stretching vibration and asymmetric stretching vibration of -C-O-C- in the lipid chain. Upon the HA coating (Figure 1D, curve d), a significant increase in the peaks intensity at the 3418 cm^{-1} and 1630 cm^{-1} region was observed, which is the result of the abundant amount of -OH and -NH_2 from HA. Furthermore, peak originating from C-OH stretching of HA at 1067 cm^{-1} was observed. Interestingly, due to the coverage of HA, both peaks (1257 cm^{-1} and 1027 cm^{-1}) corresponding to -C-O-C- in PEG disappeared.

Energy-dispersive spectroscopy (EDS) data (Figure S3) of Fe_3O_4@Au@PEG@HA NPs shows the existence of Fe, Au, C, O and N elements in the sample. Simultaneously, VSM analysis (Figure S4) again proves the fact of the successful construction of magnetic NPs steps by steps.

3.3. Antifouling performance of Fe_3O_4@Au@PEG@HA NPs modified sensor

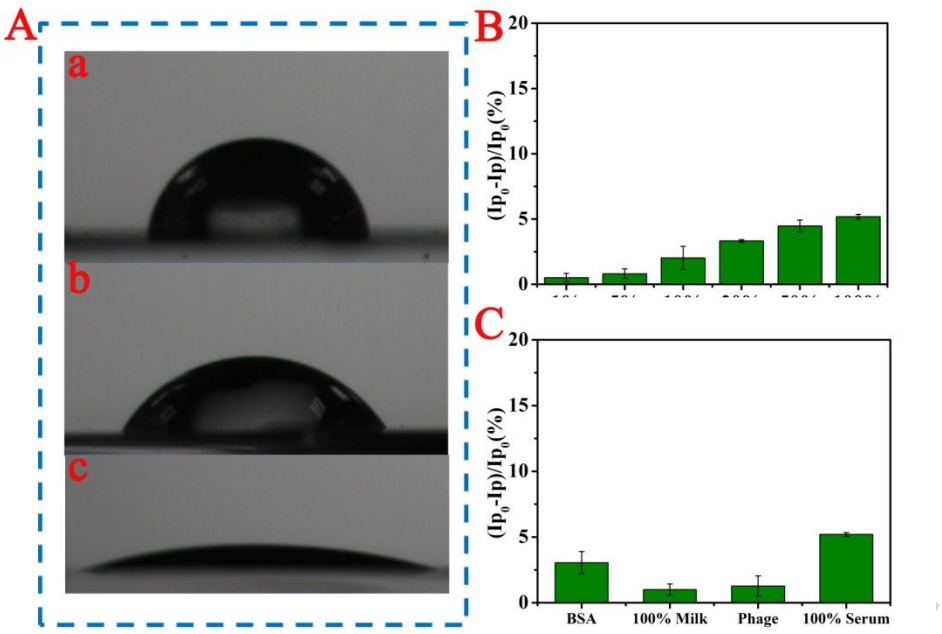

Figure 2. A: static water contact angle values of (a) bare ITO, (b) ITO/Fe_3O_4@Au@PEG NPs (c) ITO/Fe_3O_4@Au@PEG@HA NPs; B: DPV response changes of sensor constructed with Fe_3O_4@Au@PEG@HA NPs to different concentrations of serum (1 %, 5 %, 10 %, 20 %, 50 %, 100 % V/V serum). C: DPV responses changes of sensor constructed with Fe_3O_4@Au@PEG@HA NPs to different media (10 mg mL^{-1} BSA, 100 % cow milk, 1.0×10^8 pfu mL^{-1} M13KO7 and 100% serum). Error bars represent the standard deviations of three repeated determinations (n = 3).

To evaluate the protein-resistant performance of sensor constructed with Fe_3O_4@Au@PEG@HA NPs, the DPV responses of the modified electrodes were compared before and after soaking in different concentration serum (V/V, 1 %, 5 %, 10 %, 20 %, 50 %, 100 %). As shown in Figure 2B, the percent change of DPV current [$(Ip_0\text{-}Ip)/Ip_0$ (%)] ranges from 0.51% to 5.19%.

Next, more biological complex media were chosen to further evaluate the

protein-resistant performance of sensor modified by Fe_3O_4@Au@PEG@HA NPs. Figure 2C shows that the percent change of DPV current of sensor caused by the nonspecific adsorption from BSA (10 mg mL^{-1}), helper phage (M13KO7, 1×10^8 pfu mL^{-1}) and 100 % cow milk (~30 mg mL^{-1} protein) were 3.05%, 1.0% and 1.27%, respectively. All of facts prove that the interface platform of sensor possesses the excellent protein-resistant performance.

It is well known that hydration layers formed on hydrophilic surfaces is a key factor to resist nonspecific protein adsorption. (Prime and Whitesides, 1993; Schwierz at al., 2012) A static contact angle is commonly used to evaluate the surface hydrophilicity. As shown in Figure 2A, the water contact angle of bare ITO is 78.1°, when Fe_3O_4@Au@PEG@HA NPs are modified on the ITO surface, it is sharply reduced to 11.34°. Those obvious decreases may be attributed to presence of a large number of C-O-C, -OH, CO-NH and -COOH originating from PEG and HA. In addition, a phenomenon we need to emphasize is that the water contact angle of Fe_3O_4@Au@PEG NPs modified ITO surface is 58.1°, which is five times larger than that of Fe_3O_4@Au@PEG@HA NPs. This result can indirectly confirm the contribution of the fusion of HA to the antifouling performance of sensor interface.

3.4. Electrochemical characterization of the brucellosis immunosensor

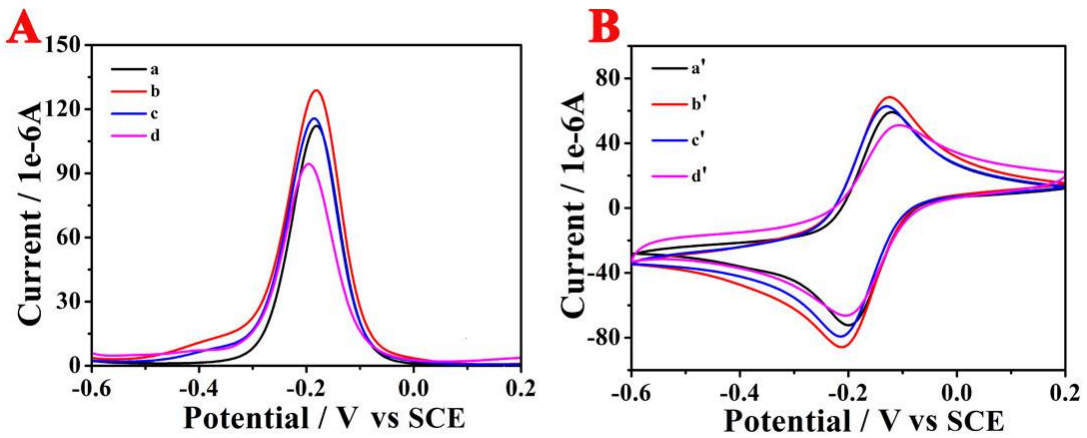

Figure 3. (A) DPV and (B) CV recorded in PBS (10 mM, pH 7.4) solution containing 5.0 mM $Ru(NH_3)_6^{3+}$ and 0.1 M KCl: (a)(a′) bare MGCE; (b)(b′) MGCE/ Fe_3O_4@Au@PEG@HA NPs; (c)(c′) MGCE/Fe_3O_4@Au@PEG@HA NPs/OMP31; (d)(d′) MGCE/Fe_3O_4@Au@PEG@HA NPs/OMP31/brucellosis antibody (10^{-11} g mL^{-1}).

Cyclic voltammetry (CV) and differential pulse voltammetry (DPV) are valuable and facile techniques for characterizing the step-by-step fabrication procedure of the immunosensor, as shown in Figure 3. A representative DPV curve was observed for the bare MGCE (Figure 3A, curve a), and there was a significant increase in the peak currents when the Fe_3O_4@Au@PEG@HA NPs were modified on the MGCE (Figure 3A, curve b), which can be expressed as a synergistic effect of the increases of surface area (Wang et al., 2018) and the enhancement of electrical conductivity. After the immobilization of OMP31, a dramatic decline in the DPV peak currents was observed (Figure 3A, curve c) due to the poor conductivity of protein which can prevent the electron transfer to some degree. Then, the DPV signal further decreased when the immunosensor was incubated with the antibody of brucellosis (Figure 3A, curve d). The similar

results (current peak change trend) were observed from CV (Figure 3B), further confirming the successful fabrication of the immunosensor.

3.5. Sensing response of the brucellosis immunosensor

The optimal incubation time for the brucellosis antibody detection with the fabricated brucellosis immunosensor was surveyed with DPV. As shown in Figure S6, the DPV current peak increased from 15 min to 60 min, then reached nearly constant, which indicates that the equilibrium time of specific binding between antigen and antibody is 60 min. Therefore, 60 min was selected as the optimal incubation time for the brucellosis immunosensor.

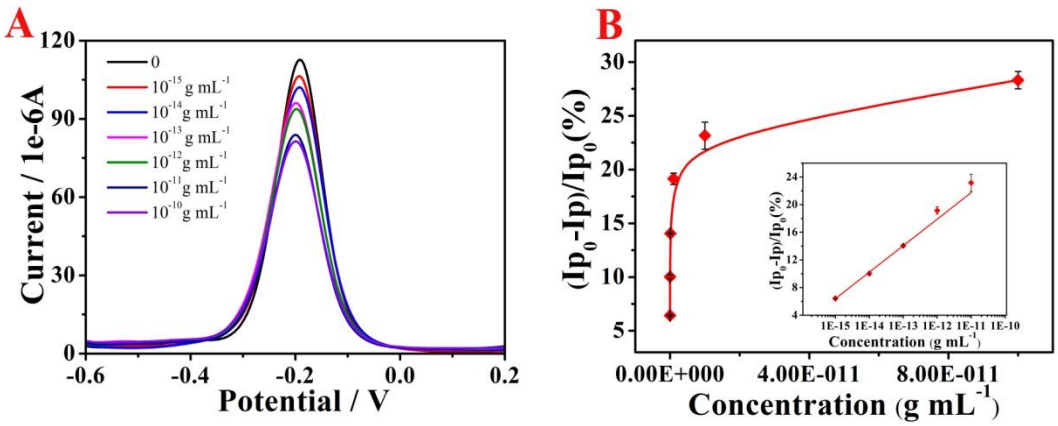

Figure 4. A: DPV responses of the immunosensor toward different concentrations of brucellosis antibody from 10^{-15} to 10^{-10} g mL^{-1} in 100 % serum; B: the dynamic response range of the immunosensor, the inset is the calibration curve of immunosensor. Error bars represent the standard deviations of three repeated determinations (n = 3).

The analytical performance of the brucellosis immunosensor for detecting brucellosis antibody was investigated in 100 % serum (Figure 4A) or in PBS (Figure S7) containing a series of brucellosis antibody concentrations using DPV. As shown in

Figure 4A, the DPV current response of the immunosensor decreased along with the increase of the brucellosis antibody concentration owing to the specific binding between antigen and antibody. The percentage of DPV peak current changes [$(Ip_0\text{-}Ip)/Ip_0$ (%)] had a linear relationship with the logarithm values of the target concentrations within the range from 10^{-15}g mL^{-1} to 10^{-11} g mL^{-1} (Figure 4B, inset). The corresponding regression equation was [$(Ip_0\text{-}Ip)/Ip_0$ (%)] = 63.93 + 3.84 log C (g mL^{-1}) with the correlation coefficient (R^2) of 0.998, and the limit of detection (LOD) was 0.36 fg mL^{-1} (3σ, n=13), which is much lower than previous report (Table S1). This analysis patterns was basically consistent with that in PBS buffer, which again confirmed that Fe_3O_4@Au@PEG@HA NPs-modified interface had the excellent protein-resistance property.

3.6. Selectivity and reproducibility of immunosensor

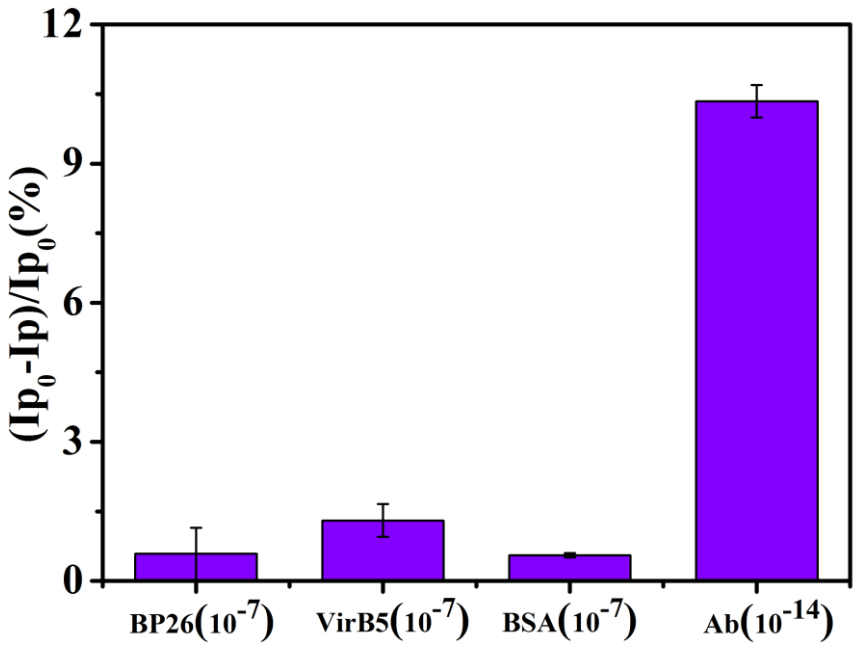

Figure 5. DPV responses changes of the immunosensor to 10^{-7} g mL^{-1} BP26, VirB5, BSA and 10^{-14} g mL^{-1} brucellosis antibodies (Ab), respectively. Error bars represent

the standard deviations of three repeated determinations (n = 3).

Due to the complexity of the component of the biological sample, the selectivity of immunosensor is crucial for their use in disease detection. The current response [(Ip_0-Ip)/Ip_0 (%)] of the immunosensor was assessed in different solutions, including BP26 (10^{-7} g mL^{-1}), VirB5 (10^{-7} g mL^{-1}), bovine serum albumin (BSA, 10^{-7} g mL^{-1}) and brucellosis antibody (10^{-14} g mL^{-1}). As shown in Figure 5, the immunosensor showed remarkable signal response to brucellosis antibody and almost no response to nonspecific proteins (BP26, VirB5 and BSA), although concentration of nonspecific protein is 10^7 times higher than that of brucellosis antibody. The excellent selectivity may be the full embodiment of the antifouling property of sensor based on Fe_3O_4@Au@PEG@HA NPs and the strong bio-affinity between OMP31 antigen and brucellosis antibody.

To evaluate the reproducibility of the immunosensor, five electrodes modified with OMP31 were used to detect 0.01 ng mL^{-1} brucellosis antibody. And it was found that the relative standard deviation (RSD) of five separate electrodes was only 2.16 %, under the same conditions. The result suggests its good reproducibility.

3.7. Analytical performance of immunosensor

The potential practical application of the brucellosis immunosensor was evaluated by quantifying a series concentration of brucellosis antibody in 100 % serum, in helper phage (M13KO7, 1× 10^{-8} pfu mL^{-1}), BSA (10 mg mL^{-1}) and 100 % cow milk (these concentrations of brucellosis antibody were far below the peak value of antibody in the actual patient's blood (10^{-7}g mL^{-1})). Before measurements, the

serum sample containing different concentrations of antibodies was prepared by the supernatants which were obtained by centrifugation of fresh blood for 10 min at 8000 rpm. The results are listed as Table S2, which shows the value of recovery ranges from 91.2% to 100.3%, and the relative standard deviation (RSD) is from 2.87 % to 4.78 %, proving the immunosensor has a promising potential in early clinical diagnosis of brucellosis. By the way, a reasonable result is also revealed in helper phage, BSA and 100% cow milk, implying the wide application performance of the immunosensor (Table S3).

4. Conclusions

In summary, a novel brucellosis immunosensor based on a new magnetic nanoparticle (Fe_3O_4@Au@PEG@HA NPs) was presented. This immunosensor exhibited a favorable selectivity, high sensitivity, a wide range of liner and ultralow detection limit, especially, an excellent antifouling property from various external environments. Interestingly, it can also be used for assaying brucellosis antibody in 100% serum, which achieved our ideal goal and also suggests the great commercial value of its clinical diagnosis.

Acknowledgments

This work was supported by the Joint Funds of the National Science Foundation of China (U1303283), National High Technology Research and Development Program of China (2015AA034602), The science and technology

project and achievement transformation plan of modern agricultural of Xinjiang Corps (2016 AC010) and The National Science and Technology Major Project (2017YFD0500304).

References

Abdel-Hamid, N. H., Ismail, R. I., Beleita, E. I. M., Ghobashy, H. M., 2017. Alexandria Journal for Veterinary Sciences 53, 11-20.

Cui, J., Ju, Y., Liang, K., Ejima, H., Lörcher, S., Gause, K. T., Richardson, J. J., Caruso, F., 2014. Soft Matter 10, 2656-2663

Cui, M., Wang, Y., Jiao, M., Jayachandran, S., Wu, Y., Fan, X., Luo, X., 2017. ACS Sens. 2, 490-494.

Dosio, F., Arpicco, S., Stella, B., Fattal, E., 2016. Adv. Drug Delivery Rev. 97, 204-236.

Feng, B., Hong, R. Y., Wang, L. S., Guo, L., Li, H. Z., Ding, J., Zheng, Y., Wei, D. G., 2008. Colloids Surf., A 328, 52-59.

Ghasemi, A., Ranjbar, R., Amani, J., Iran. 2014. J. Basic Med. Sci. 17, 172.

Ghodasara, S. N., Roy, A., Bhanderi, B. B., 2010. Vet. World 3, 61-4.

Gong, L., Dai, H., Zhang, S., Lin, Y., 2016. Anal. Chem. 88, 5775-5782.

Gref, R., Lück, M., Quellec, P., Marchand, M., Dellacherie E., Harnisch, S., Blunk, T., Müller, R. H., 2000. Colloids Surf., B 18, 301-313.

Huang, R., Liu, X., Ye, H., Su, R., Qi, L., Wang, L., He, Z., 2015. Langmuir 31, 12061-12070.

Hui, N., Sun, X., Niu, S., Luo, X., 2017. ACS Appl. Mater. Interfaces 9, 2914-2923.

Kuila, P., Dutta, D., Chakrabarty, U., Chatterjee, D., Das, S., 2017. Asian J. Pharm. Clin. Res. 10, 109-111.

Li, J., He, Y., Sun, W., Luo, Y., Cai, H., Shen, M., Xia, J., Shi, X., 2014. Biomaterials

35, 3666-3677.

Li, J., Xu, Q., Wei, X., Hao, Z., J. 2013. Agric. Food Chem. 61, 1435-1440.

Li, T., Tong, Z., Huang, M., Tang, L., Zhang, H., Chen, C., 2017. Can. J., Microbiol. 63, 719-729.

Liu, X., Huang, R., Su, R., Qi, W., Wang, L., He, Z., 2014. ACS Appl. Mater. Interfaces 6, 13034-13042.

Lyon, J. L., Fleming, D. A., 2004. Nano Lett. 4, 719-723.

Michel, R., Pasche, S., Textor, M., Castner, D. G., 2005. Langmuir 21, 12327-12332.

Mukhopadhyay, A., Joshi, N., Chattopadhyay, K., De, G., 2011. ACS Appl. Mater. Interfaces 4, 142-149.

Ostuni, E., Chapman, R. G., Holmlin, R. E., Takayama, S., Whitesides, G. M., 2001. Langmuir 18.

Prime, K. L., Whitesides, G. M., 1993. J. Am. Chem. Soc. 115, 10714-10721.

Schwierz, N., Horinek, D., Liese, S., Pirzer, T., Balzer, B. N., Hugel, T., Netz, R. R., 2012. J. Am. Chem. Soc. 134, 19628-19638.

Wang, G., Su, X., Xu, Q., Xu, G., Lin, J., Luo, X., 2018. Biosens. Bioelectron 101, 129-134.

Xie, J., Xu, C., Kohler, N., Hou, Y., Sun, S., 2007. Advanced Materials 19, 3163-3166.

Xu, Z., Hou, Y., Sun, S., 2007. J. Am. Chem. Soc. 129, 8698-8699.

Ye, H., Xia, Y., Liu, Z., Huang, R., Su, R., Qi, W., Wang, L., He, Z., 2016. J. Mater. Chem. B, 4, 4084-4091.

Yu Y, Frey, H., 2015. Langmuir 31, 13101-13106.

Zhang, Z., Chen, S., Jiang, S., 2006. Biomacromolecules 7, 3311-3315.

Zhao, J., Zhang, Y., Li, H., Wen, Y., Fan, X., Lin, F., Tan, L., Yao, S., 2011. Biosens. Bioelectron., 26, 2297-2303.

Zhao, X., Cai, Y., Wang, T., Shi, Y., Jiang, G., 2008. Anal. Chem. 80, 9091-9096.

Zheng, W. Y., Wang, Y., Zhang, Z. C., Yan, F., 2015. Genet. Mol. Res. 14, 11965-11974.

Highlights

- A novel immunosensor for detection of brucellosis was fabricated with Fe_3O_4@Au@PEG@HA NPs;
- The interface platform of immunosensor exhibited excellent antifouling property in 100 % serum;
- The immunosensor can be capable of quantifying brucellosis antibody in 100% serum.